


RESEARCH

Open Access



Cyasterone ameliorates sepsis-related acute lung injury via AKT (Ser473)/GSK3 β (Ser9)/Nrf2 pathway

Miao Lin^{1†}, Weixi Xie^{1†}, Dayan Xiong¹, Siyuan Tang¹, Xiaoting Huang¹, Lang Deng¹, Lei Huang², Xiaohua Zhang², Tingting Zhou¹, Rui Qian¹, Qian Zeng¹, Xiaoxue Sang¹, Yuyang Luo¹, Qingzhong Hua¹, Lu Ren^{3*} and Wei Liu^{1*} 

Abstract

Background Acute lung injury (ALI) is a severe disease that can lead to acute respiratory distress syndrome (ARDS), characterized by intractable hypoxemia, poor lung compliance, and respiratory failure, severely affecting patients' quality of life. The pathogenesis of ALI has not been fully elucidated yet, and sepsis is an important cause of ALI. Among the organ injuries caused by sepsis, the lungs are the earliest damaged ones. Radix cyathulae is reported to have analgesic, anti-inflammatory, and anti-aging effects. Cyasterone is extracted from Radix cyathulae. However, it is not known whether cyasterone has protective effects for ALI. This study aims to investigate the effect of cyasterone on sepsis-related ALI and its mechanism.

Methods We used the cecal ligation perforation (CLP) method to establish a mouse sepsis model, and cyasterone was given intraperitoneally on days 1–3 to observe its preventive effect on sepsis-related acute lung injury. Primary murine peritoneal macrophages were used to investigate the molecular mechanism of cyasterone in vitro.

Results Cyasterone pretreatment inhibits pro-inflammatory cytokine production, NLRP3 inflammasome activation, and oxidative stress in vivo and in vitro. In addition, cyasterone attenuates sepsis-induced ALI by activating nuclear factor erythroid2-related factor (Nrf2), which may be associated with AKT(Ser473)/GSK3 β (Ser9) pathway activation.

Conclusions Cyasterone defends against sepsis-induced ALI by inhibiting inflammatory responses and oxidative stress, which depends heavily on the upregulation of the Nrf2 pathway through phosphorylation of AKT(Ser473)/GSK3 β (Ser9). These results suggest cyasterone may be a valuable drug candidate for preventing sepsis-related ALI.

Keywords Cyasterone, Acute lung injury, Inflammation, Oxidative stress, Nrf2, AKT

[†]Miao Lin and Weixi Xie have contributed equally to this work.

*Correspondence:

Lu Ren
renlu108811@csu.edu.cn

Wei Liu
liuw079@csu.edu.cn

Full list of author information is available at the end of the article



Introduction

Sepsis, defined by the World Health Organization (WHO) as a global health priority, is characterized by excessive inflammation after infection, with a mortality rate of 30–45% in hospitalized patients [1]. ALI/ARDS is the most common form of multi-organ dysfunction syndrome and an influential driver of sepsis morbidity and mortality [2]. Due to the lack of specific drugs, mechanical ventilation remains the primary supportive treatment for ALI/ARDS [3]. However, this may cause alveolar wall damage and further induce lung injury-related mechanical ventilation [4, 5]. Therefore, developing safe and effective drugs to reduce the mortality of sepsis patients by preventing the occurrence of ALI is significant.

As heterologous phagocytes in innate immunity, macrophages detect pathogen-associated molecular patterns (PAMP) and injury-associated molecular patterns by expressing pattern recognition receptors [6]. Infiltration of macrophages and neutrophils activated by inflammatory response into the lung activates pro-inflammatory networks and promotes reactive oxygen species (ROS) release [7]. In response to increasing ROS, thioredoxin-interacting protein (TXNIP) detaches from thioredoxin (Trx), binds to nucleotide-binding structural domain-like receptor protein 3 (NLRP3), and then activates NLRP3 inflammasome [8]. The activation of NLRP3 inflammasome further leads to the maturation and release of pro-inflammatory cytokines, such as interleukin-1 β (IL-1 β), tumor necrosis factor- α (TNF- α) and induces oxidative stress [9].

Nrf2 plays a critical role in many inflammatory and oxidative stress-related diseases [10], and it regulates almost all Nrf2 antioxidant response element (ARE) signals transcriptionally [11]. Kelch-like ECH-associated protein 1 (Keap1) is a repressor protein that binds to Nrf2 and promotes its degradation via the ubiquitin–proteasome pathway, a major regulator pathway of Nrf2 [12]. In addition to keap1-dependent Nrf2 regulation, growing evidence suggests that the GSK-3 β -mediated regulatory pathway independent of keap1 is a crucial route for Nrf2 activation and, thus, protection against multifunctional organ damage [13].

Radix cyathulae is a traditional herb that promotes blood circulation, strengthens bones and muscles, and is known for its analgesic, anti-inflammatory, and anti-aging benefits [14–16]. Cyasterone is extracted from Radix cyathulae [17, 18]. Considering the known anti-inflammatory effects of cyasterone [19, 20], and the limitations of the current treatment of sepsis-related ALI, we investigated the protective effect of cyasterone against CLP-induced ALI and its mechanism.

Materials and methods

Animals

C57BL/6 mice (male, 6–8 weeks) were purchased from the Animal Center of Central South University and housed under specific pathogen-free conditions. After a week of adaptive feeding, to observe the preventive effect of cyasterone, mice were divided into five groups randomly: control, CLP, CLP+L, CLP+M, and CLP+H group. Mice were injected intraperitoneally (i. p.) with cyasterone (1, 5, or 25 mg/kg/d) for 3 days. To verify the preventive effect of cyasterone, the mice were randomly divided into five groups: control, CLP, CLP+M, CLP+M+ML385, and CLP+M+LY294002. Mice were injected intraperitoneally (i. p.) ML385 (30 mg/kg/d, selleck, China) or LY294002 (5 mg/kg/d, selleck, China) for 3 h following administration intraperitoneally (i. p.) with cyasterone (5 mg/kg/d) for 3 days. To compare the drug effects of cyasterone and the positive drug dexamethasone, mice were divided into four groups randomly: control, CLP, CLP+M, and CLP+DEX. Mice were injected intraperitoneally (i. p.) with cyasterone (5 mg/kg/d) or dexamethasone (5 mg/kg/d) for 3 days [21, 22]. Cyasterone (Cat#: S9414, Selleck, China) was diluted with 0.9% saline, containing 40% PEG300 (Macklin, China), 5% dimethyl sulfoxide (DMSO) (Macklin, China), and 5% Tween80 (Macklin, China) (v/v/v). This study was conducted following the welfare and ethical principles of experimental animals. It was approved by the Laboratory Animal Welfare and Ethical Committee of Central South University (Approval No. CSU-2022-0095).

CLP model

Mice were fasted for 12 h prior to surgery. After anesthesia, the skin was disinfected, and the cecum was exposed by making a 1 cm incision toward the middle of the abdomen of the mice. The cecum was ligated with 4–0 braided silk thread through the midpoint between the root and the end of the cecum. A 21-gauge needle was inserted into the ligated cecum, and a small drop of intestinal contents was extruded to induce infection. Finally, the cecum was reset, and the incision was closed [23]. For the control group, the abdomen was opened, and then the incision was closed. 24 h later, lung tissue or bronchoalveolar lavage fluid (BALF) was obtained for subsequent experiments.

Histopathological evaluation

The right mid-lung of the mice was fixed, embedded in 4% paraformaldehyde neutral buffer overnight, cut into 4 μ m sections, and stained with hematoxylin–eosin [24]. The severity of the injury was graded from 0 to 5:

alveolar wall intact without thickening, no inflammatory infiltrate, no congestion, 0; alveolar wall thickening, slight inflammatory cell infiltration, 1; alveolar wall thickening, slight inflammatory cell infiltration, capillary dilation, 2; alveolar wall thickening significantly, inflammatory cell infiltration, interstitial congestion, 3; alveolar wall thickening, severe inflammatory cell infiltration, diffuse distribution, destruction of alveolar structure, necrosis and decompensation of bronchial mucosa epithelial cells, and solidification of lung tissue, 4; the alveolar wall thickening, severe inflammatory cell infiltration, diffuse distribution, destruction of alveolar structure, and solidification of lung tissue, 5. The inflammation score was measured independently by three pathologists blinded to the experiment.

Lung wet to dry (W/D) ratio

The left lung was removed and weighed on a precision electronic scale (BSA224S-CW; sartorius, Germany), then placed in an oven and baked at 56 °C for 48 h until a constant weight was obtained as dry weight. The W/D ratio was calculated to evaluate the degree of pulmonary edema.

M1 macrophage activation

The proportion of M1 macrophages in BALF was determined by flow cytometry. Cells were stained with PE-conjugated anti-mouse F4/80 (Cat# E-AB-F0995UD, Elabscience, China), APC-conjugated anti-mouse CD80 (Cat# E-AB-F0992E, Elabscience, China), and FITC-conjugated anti-mouse CD11b (Cat# E-AB-F1081C, Elabscience, China). Briefly, F4/80 is employed for labeling macrophages in BALF, while CD80 is utilized for marking M1-type macrophages.

Enzyme-linked immunosorbent assay (ELISA)

BALF was captured by 2 intratracheal injections of 0.8 ml of cooled phosphate buffered saline (PBS). BALF was centrifuged at 4 °C for 10 min at 1500 r/min, lysed in ACK lysis buffer for 5 min, washed twice with ice-cold PBS, and centrifuged for 5 min. Subsequently, the contents of tumor necrosis factor-alpha (TNF- α) and interleukin-1 beta (IL-1 β) in BALF were measured using ELISA kits (Cat# TNF- α : 88-7324; IL-1 β : 88-7013; Invitrogen, USA). The contents were assayed by comparison of the optical density (450 nm) with the standard curve [25].

Measurement of MPO, MDA, GSH and SOD levels

Lung tissues were lysed in extraction buffer, and all procedures were conducted strictly according to the instructions of superoxide dismutase (SOD), myeloperoxidase (MPO), glutathione (GSH) and

malondialdehyde (MDA) assay kits (Cat# SOD: A001-3-2; MPO: A044-1-1; GSH: A006-2-1; MDA: A003-1-2; Nanjing Jiancheng Bioengineering Institute, Nanjing, China).

Cells culture

Primary murine peritoneal macrophages were isolated from C57BL/6 mice. Mice were injected with 3 ml of 3% thioglycolate (Sigma-Aldrich, St. Louis, MO, USA). 4 days later, peritoneal macrophages were obtained by intraperitoneal lavage with prechilled RPMI 1640 (Procell, Wuhan, China). Cells were collected and centrifuged at 1500 rpm for 10 min at 4 °C, and the precipitate was resuspended in RPMI 1640. Cells were placed in 6-well plates (2×10^6 cells/well) for protein detection and ROS assessment, 12-well plates (1×10^6 cells/well) for RNA detection, and 24-well plates (0.5×10^6 cells/well) for immunofluorescence staining. After 2 h, RPMI 1640 containing 10% neonatal bovine serum (NBS, Sigma, USA) and 1% streptomycin/penicillin (Gibco, Waltham, MA, USA) were replaced, and non-adherent cells were removed. Cells were cultured in a humidified CO₂ incubator at 37 °C. MLE-12 cells (provided by the State Key Laboratory of Genetics, Changsha) were cultured with 100 U/ml of streptomycin/penicillin and fetal bovine serum (10%) in DMEM (Gibco, USA) and arranged in an incubator containing 5% CO₂ with a suitable temperature (37 °C).

All cells were incubated with cyasterone (10 μ M, 30 μ M or 100 μ M) for 24 h before being stimulated with or without LPS (100 ng/ml, from *Escherichia coli* O111: B4, Sigma-Aldrich, USA) according to different requirements.

CCK-8 assay

Cell viability was assayed with Cell Counting Kit-8 (CCK-8) (Dojindo, Kumamoto, Japan). Primary murine peritoneal macrophages and MLE12 cells were incubated on 96-well plates and treated with different concentrations of cyasterone (1 μ M, 3 μ M, 10 μ M, 30 μ M, 100 μ M, 200 μ M). After 24 h, 10 μ l CCK-8 reagent was added to each well and incubated at 37 °C for 1 h. OD values were measured by 450 nm enzyme assay.

Measurement of MDA, GSH and SOD levels

Primary peritoneal macrophages were lysed in extraction buffer, and all procedures were conducted strictly according to the instructions of superoxide dismutase (SOD), myeloperoxidase (MPO), glutathione (GSH) and

malondialdehyde (MDA) assay kits (Cat# SOD: A001-3-2; MPO: A044-1-1; GSH: A006-2-1; MDA: A003-1-2; Nanjing Jiancheng Bioengineering Institute, Nanjing, China).

Measurement of ROS content

Primary peritoneal macrophages and MLE12 cells were incubated with 20 μM 2',7'-Dichlorodihydrofluorescein diacetate (DCFH-DA) (Thermo, D399) for 30 min at 37 °C in the dark and washed three times with pre-cooled PBS. Fluorescence microscopy (Nikon Ti-s, Tokyo, Japan) and flow cytometry (BD LSRFortessa, Franklin Lakes, NJ, USA) were performed to observe the production of ROS.

The apoptosis assay

Apoptosis assays were performed using the Annexin V-FITC Apoptosis Detection Kit (Cat# C1062L, Beyotime, China) according to the manufacturer's instructions. Briefly, MLE12 cells were washed twice with cold PBS and resuspended in PBS at a concentration of 1 × 10⁶ cells/ml. Subsequently, cells were stained with 5 μl of FITC Annexin V and 5 μl of propidium iodide, and incubated at room temperature in the dark for 15 min. Finally, the samples were analyzed using flow cytometry (BD LSRFortessa, Franklin Lakes, NJ, USA), and the results were analyzed using Flowjo10 software.

Real-time quantitative polymerase chain reaction (Q-PCR)

Total RNA from lung tissues and cells was extracted with TRIzol (Thermo Fisher Scientific, USA) and reverse transcribed into cDNA using a reverse transcription kit (Thermo Fisher Scientific, USA) in accordance with the manufacturer's protocol. Q-PCR was performed using SYBR GREEN (Promega, USA) and Bio-Rad CFX96 Touch Real-Time PCR Detection System (Bio-Rad, USA) Q-PCR. PCR conditions were as follows. 95 °C for 2 min,

followed by 40 cycles of 95 °C for 3 s and 60 °C for 30 s, plus a 60–95 °C melting curve. Data were expressed in C.T. values normalized to β-actin, and the fold change between control and treated groups was determined using the 2-ΔΔCt method. The sequences are shown in Table 1.

Western blot analysis

Lung tissue and cells were plunged in ice-cold RIPA lysis buffer with protease and phosphatase inhibitors (Abcam, Cambridge, UK). Per the manufacturer's instructions, protein concentrations were quantified using the BCA Protein Assay Kit (Beyotime Biotech, Shanghai, China). Briefly, protein samples were loaded and separated on SDS-PAGE gels, transferred to PVDF membranes (Bio-Rad, USA), and blocked with 5% (w/v) skimmed milk containing 0.1% PBS buffer Tween 20 (v/v) or 5% (w/v) protease free bovine serum Albumin (BSA) (Sigma-Aldrich, USA). Then the membranes were incubated with β-actin antibody (1:5000, Cat#: 81,115-1-RR, SAB), NLRP3 anti-body (1:2000, Cat#: 15,101, CST), pro-caspase-1/p10/p20 antibody (1:1000, Cat#: ab179515, Abcam), Heme Oxygenase 1 antibody (1:1000, Cat#: ab52947, Abcam), NQO1 antibody (1:3000, Cat#: ab80588, Abcam), p-GSK3β (S9) antibody (1:1000, Cat#: WL03518, WanleiBio), GSK3β antibody (1:300, Cat#: WL01456, WanleiBio), p-AKT (Ser473) antibody (1:500, Cat#: WLP001a, WanleiBio), AKT antibody (1:500, Cat#: WL0003b, WanleiBio) overnight at 4 °C, and secondary antibodies (1: 5000, SAB) were labeled with horseradish peroxidase for 2 h at room temperature. After washing with PBST, bands were detected with Luminata™ Crescendo chemiluminescence horseradish peroxidase substrate (Millipore, USA) and scanned using GeneGnome XRQ imager (Syngene, UK).

Table 1 Primer sequences for qPCR

Gene	Forward primer	Reverse primer
β-actin	GGCTGTATTCCCCTCCAT	CCAGTTGGTAACAATGCCATGT
HO-1	ACCGCCTTCTCTCAACATTG	CTCTGACGAAGTGACGCCATCTG
NQO-1	GCGAGAAGAGCCCTGATTGTACTG	AGCCTCTACAGCAGCCTCCTTC
NLRP3	TACGGCCGTCTACGTCTTCT	CGCAGATCACACTCCTCAAA
ASC	GACAGTACCAGGCAGTTTCTG	AGTCCTTGCCAGGTCAGGTTT
Pro-caspase-1	CACAGCTCTGGAGATGGTGA	CTTTCAAGCTTGGGCACCTT
IL-6	CTTCTGGGACTGATGCTGGTGAC	AGGTCGTGGGAGTGGTATCCTC
IL-1β	TCCGAGCAGCATCAACAAGAG	AGGTCCACGGAAAGACACAGG
TNF-α	GCCTCTCTCATTCCTGCTTGTGG	GTGGTTTGTGAGTGTGAGGGTCTG

Immunofluorescence

Primary peritoneal macrophages were fixed in 4% paraformaldehyde for 15 h, permeabilized with 0.5% (v/v) Triton X-100 for 20 min, blocked with goat serum (ZSGB Bio, China) for 30 min, and then incubated with Nrf2 antibody (1:100, Proteintech, China) overnight at 4 °C. After washing with PBST, samples were incubated with fluorescent secondary antibody (1:100, Proteintech, China) in PBST for 1 h at room temperature, and DAPI was used to stain cell nuclei for 5 min and observed under the fluorescence microscope (Nikon Ti-s, Tokyo, Japan).

Statistical analysis

All experiments were independently repeated three times. All data were presented as means ± standard deviations and analyzed using GraphPad Prism 9.0. A one-way analysis of variance and Student-Newman-Kersee (SNK) tests were used to compare the groups. P value < 0.05 was defined as a statistically significant difference.

Results

Cyasterone attenuates inflammation and oxidative stress in CLP-induced ALI mice

To explore whether cyasterone can attenuate CLP-induced ALI in mice. The mice were intraperitoneally injected with different concentrations of cyasterone. CLP surgery was performed 1 h after cyasterone injection. 24 h later, the lungs and BALF were collected for subsequent experiments (Fig. 1A). HE staining was applied to appraise the pathological changes in lung tissues. The results showed alveolar wall thickening, interstitial inflammatory cell infiltration, and alveolar collapse in the CLP group mice (Fig. 1B, C). Notably, cyasterone attenuated these pathological changes (Fig. 1B, C) and reduced the lung wet/dry ratio (Fig. 1D). Macrophage count and flow cytometry results in BALF showed that macrophages were significantly elevated in the CLP group, and most of them were M1-type macrophages. In contrast, cyasterone pretreatment reduced the number of macrophages and inhibited M1-type macrophage activation (Fig. 1E–G). Next, we evaluated the effect of cyasterone on the degree of inflammation in ALI mice. The results showed that cyasterone pretreatment significantly reduced the expression of inflammatory factors in lung tissues and BALF (Fig. 1H, I, J–M) and inhibited the activation of NLRP3 inflammasome in lung tissues (Fig. 1N–R). Oxidative stress is one of the characteristics of ALI [26]. Cyasterone pre-treatment also inhibited the MPO activity, decreased the MDA

content, increased the GSH content and restored the antioxidant enzyme SOD activity in lung tissues (Fig. 1S–V). In addition, our results showed that cyasterone pre-treatment promoted the expression of NQO-1 and HO-1 (Fig. 1W–Z). These results suggest that cyasterone attenuates the inflammation and increases antioxidant capacity in CLP-induced ALI mice. Further, the effects of cyasterone and dexamethasone in the prevention of ALI were compared, the results demonstrate that cyasterone and dexamethasone are capable of alleviating CLP-induced ALI. The differences in their effects do not hold statistical significance (Additional file 1: Fig. S1).

Cyasterone inhibits the activation of NLRP3 inflammasome in primary murine macrophages

To investigate the effect of cyasterone on LPS-induced NLRP3 activation in primary murine macrophages. Cells were treated with different doses of cyasterone (0, 1, 3, 10, 30, 100 and 200 μM) for 24 h. Results showed that cyasterone (1, 3, 10, 30, 100 and 200 μM) was not toxic to cells (Fig. 2A). We proceeded to appraise the efficacy of cyasterone on the inflammatory response of primary mouse macrophages and found that low doses of cyasterone (10 μM) had no significant effect on the expression of pro-inflammatory factors (Fig. 2B–E). However, cyasterone (30, 100 μM) pretreatment significantly reduced LPS-induced inflammatory factor expression, including IL-6, IL-1β, TNF-α, and COX-2 (Fig. 2B–E). Importantly, cyasterone pretreatment inhibited NLRP3 inflammasome activation (Fig. 2F–J). These results imply that cyasterone inhibits the activation of NLRP3 inflammasome in vitro.

Cyasterone reduces oxidative stress in primary murine macrophages

ROS is among the most critical factors regulating NLRP3 inflammasome activation [9]. After LPS stimulation of cells, we measured intracellular ROS content. Both immunofluorescence and flow cytometric results found that cyasterone facilitated the subsidence of ROS (Fig. 3A–D). Cyasterone also reduced MDA content, increased GSH content and restored SOD activity in macrophages (Fig. 3E–G). Together, these results demonstrate that cyasterone attenuates oxidative stress levels in vitro.

Cyasterone exerts anti-inflammatory and oxidative stress effects by activating Nrf2 in primary murine macrophages

Nrf2 transcriptionally regulates almost all antioxidant response element (ARE) pathways [11]. Therefore, we examined the effect of cyasterone on Nrf2 nuclear

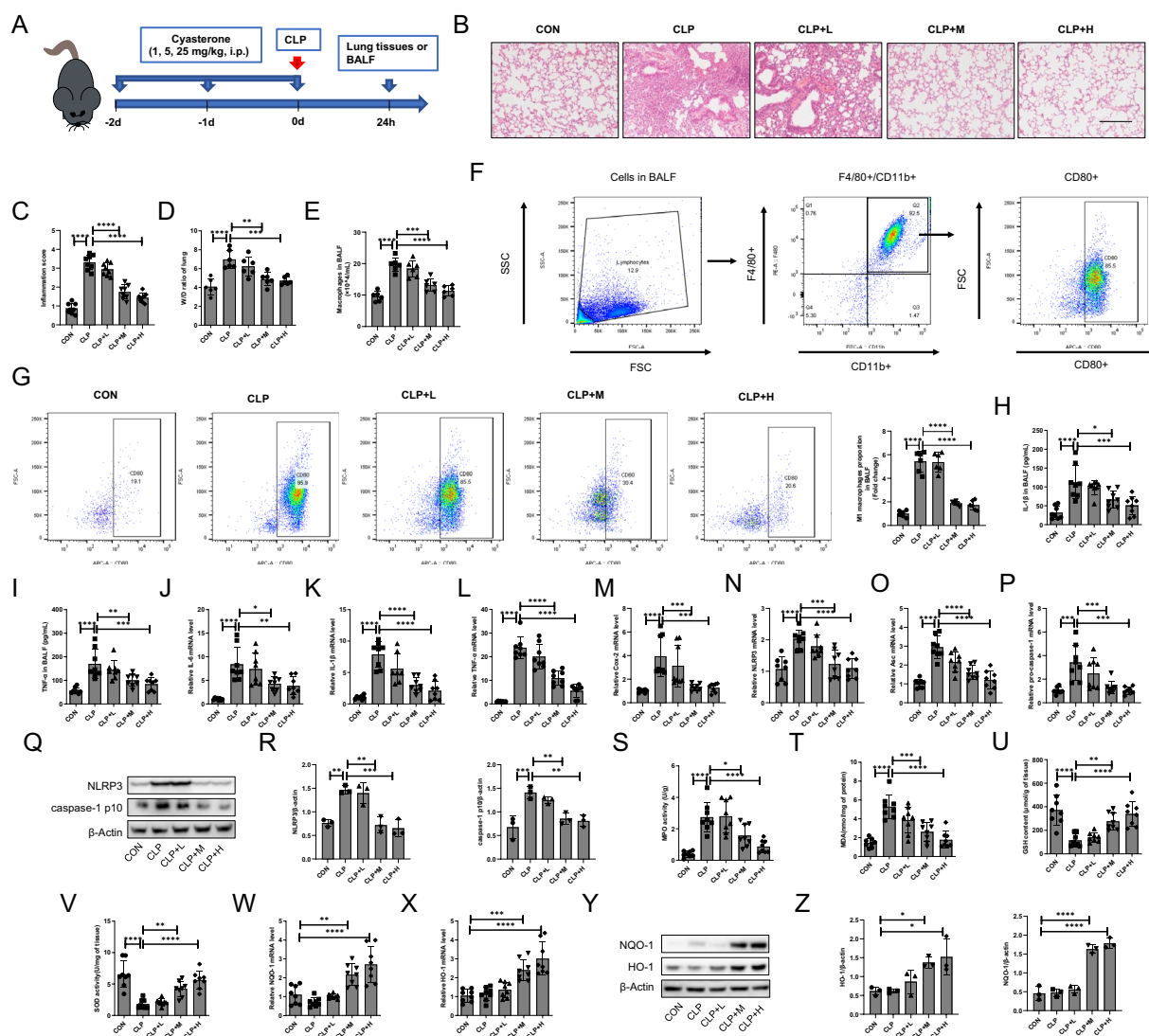


Fig. 1 Cyasterone attenuates inflammation and oxidative stress in CLP-induced ALI mice. **A** Cyasterone was administered intraperitoneally at high (25 mg/kg), moderate (5 mg/kg), and low (1 mg/kg) doses to evaluate its prevention effects on CLP-induced ALI. **B**, **C** HE staining and lung inflammation score were used to detect the lung histopathological changes. Bars represent 100 μ m. **D** Lung W/D ratio was measured to determine lung permeability. **E** The number of macrophages in BALF was measured. **F** The diagram of M1 Macrophage Cell Screening. **G** Flow cytometry was used to analyze and quantify the amount of CD80, an M1 macrophage marker in BALF. **H**, **I** IL-1 β , TNF- α in BALF were determined with ELISA. **J**–**P** IL-6, IL-1 β , TNF- α , Cox2, NLRP3, pro-caspase-1 and Asc mRNA in the lungs were determined with Q-PCR. **Q**, **R** Western blotting was used to detect the protein expression levels of NLRP3 and caspase-1 p10. **S**, **V** MPO activity, MDA content, GSH content and SOD activity in lung tissue were determined. **W**–**Z** Q-PCR and Western blotting were used to detect the mRNA and protein expression levels of NQO-1 and HO-1. Data are expressed as mean \pm SD, n = 6–8, *P < 0.05; **P < 0.01; ***P < 0.001; ****P < 0.0001

trans-location and showed that cyasterone facilitated Nrf2 entry into the nucleus concentration-dependently (Fig. 4A). It was shown that cyasterone could promote the mRNA and protein expression of Nrf2 downstream antioxidant enzymes NQO1 and HO-1 (Fig. 4B–E). After intervention with ML385 (Nrf2 inhibitor), we revealed

that the role of cyasterone in inhibiting oxidative stress (Fig. 4F–I), reducing the expression of inflammatory factors (Fig. 4J–M), and suppressing NLRP3 inflammatory activation (Fig. 4N–R) were reversed to some extent. These results suggest that cyasterone

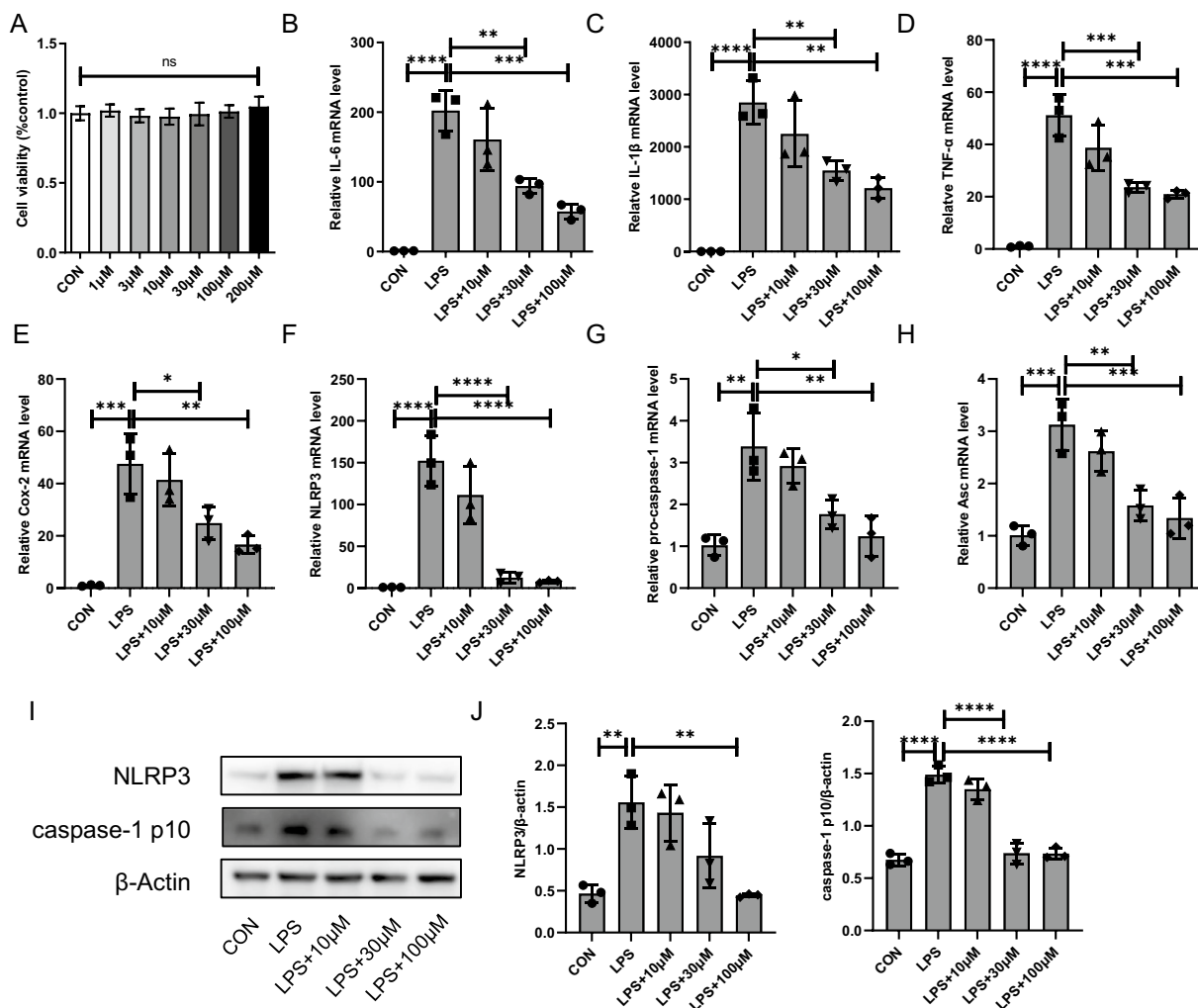


Fig. 2 Cyasterone inhibits the activation of NLRP3 inflammasome in primary murine macrophages. **A** The effects of the different concentrations of cyasterone (0, 1, 3, 10, 30, 100 and 200 µM) on cell viability were evaluated. **B–J** Primary murine macrophages were treated with serial concentrations of cyasterone (10, 30 and 100 µM) for 24 h with or without LPS (100 ng/ml) for 12 h. **B–H** IL-6, IL-1β, TNF-α, Cox2, NLRP3, pro-caspase-1 and Asc mRNA were determined with Q-PCR. **I, J** Western blotting was used to detect the protein expression levels of NLRP3 and caspase-1 p10. Data are expressed as mean ± SD, n = 3, *P < 0.05; **P < 0.01; ***P < 0.001; ****P < 0.0001

inhibits NLRP3 inflammasome activation and promotes ROS clearance in macrophages by activating Nrf2.

The AKT (Ser473)/GSK3β (Ser9) pathway mediates cyasterone-induced Nrf2 activation in primary murine macrophages

Various upstream signals can activate Nrf2 [27–29]. In this study, we explored the role of inhibitors of five essential kinases upstream of Nrf2, SIRT1, AMPK, AKT, PDK and PKA in the antioxidant and anti-inflammatory activities of cyasterone. Cells were pre-dressed by using

the kinase inhibitors EX527, Compound C, LY294002, GSK2334470 and H89, respectively, and the results showed that LY294002 inhibits the mRNA levels of NQO-1 and HO-1 (Fig. 5A–D). Cyasterone could promote the phosphorylation of AKT Ser473 (activation) and GSK3β Ser9 (inactivation) in a time-dependent manner (Fig. 5E, F). The results further showed that both antioxidant and anti-inflammatory effects of cyasterone were inhibited after the inhibition of AKT (Fig. 5G–S). Taken together, the results suggest that cyasterone promotes Nrf2 into the nucleus via AKT (Ser473)/GSK3β

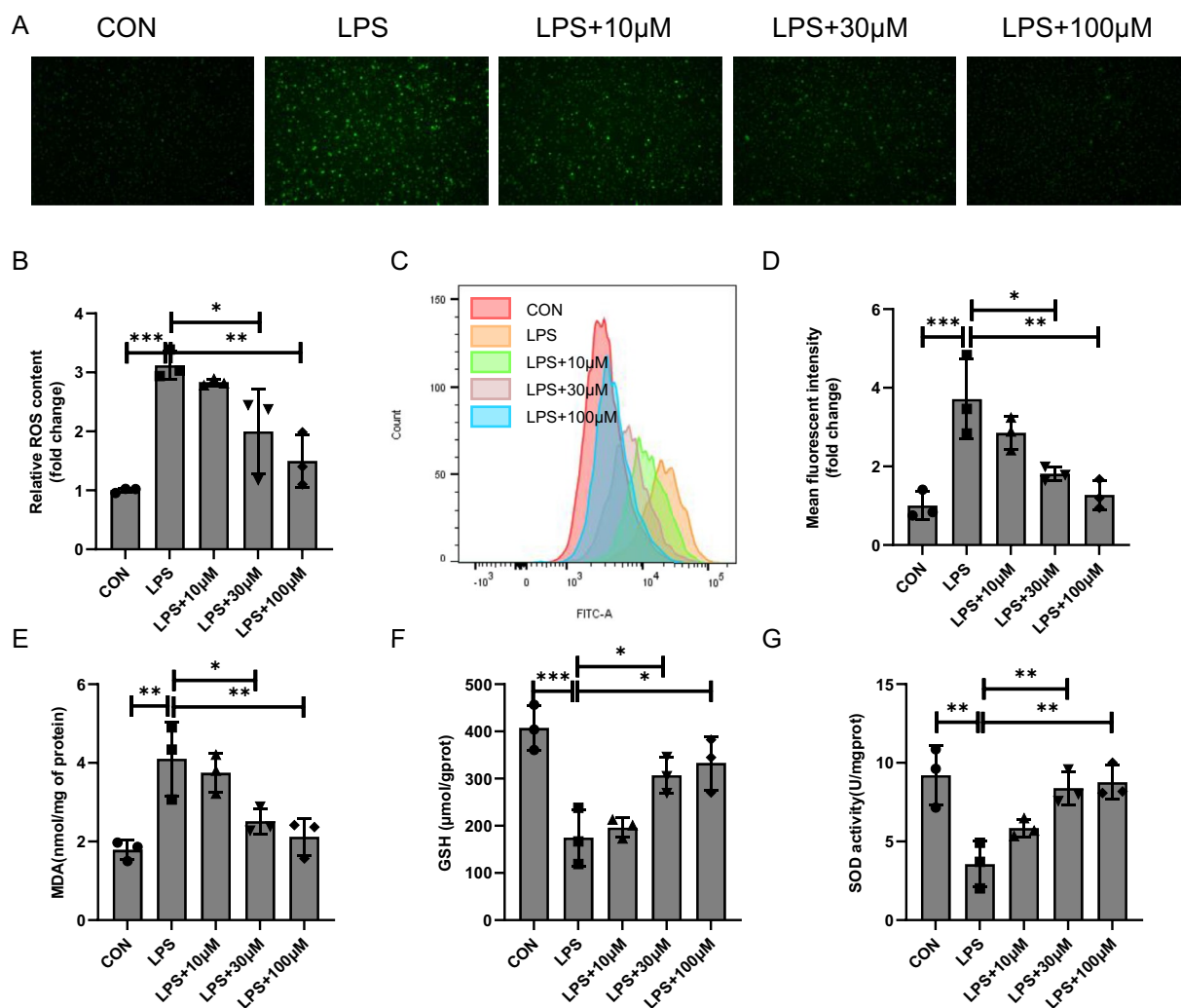


Fig. 3 Cyasterone reduces oxidative stress in primary murine macrophages. Primary murine macrophages were treated with serial concentrations of cyasterone (10, 30 and 100 µM) for 24 h with or without LPS (100 ng/ml) for 12 h. **A, B** The ROS content was analyzed by fluorescence microscopy. **C, D** The ROS content was measured by flow cytometry. **E–G** MDA content, GSH content and SOD activity in macrophages were determined. Data are expressed as mean ± SD, n = 3, *P < 0.05; **P < 0.01; ***P < 0.001; ****P < 0.0001

(Ser9) pathway, thereby inhibiting inflammation and oxidative stress.

Cyasterone against oxidative damage and apoptosis in MLE12 cells

Given the role exerted by cyasterone in peritoneal macrophages, we proceeded to investigate the antioxidative capability of cyasterone in MLE12 cells. We initiated by assessing the impact of cyasterone (1,

3, 10, 30, 100 and 200 µM) on cell viability, and the CCK assay indicated that cyasterone did not inflict damage on MLE12 cells (Fig. 6A). Subsequently, after pre-treating the cells with cyasterone for 24 h followed by a 12h LPS stimulation, both immunofluorescence and flow cytometry results demonstrated that cyasterone (30, 100 µM) managed to reduce cellular and mitochondrial ROS levels (Fig. 6B–D). Notably, the JC-1 assay exhibited a concentration-dependent increase in the proportion of LPS-induced JC-1

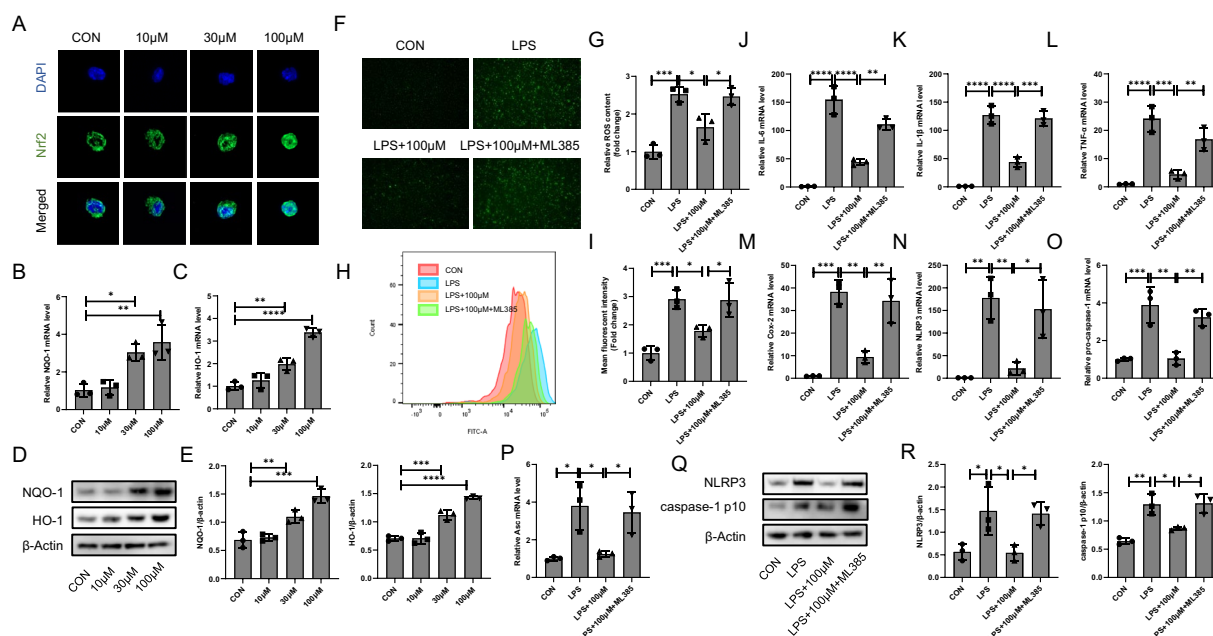


Fig. 4 Cyasterone exerts anti-inflammatory and oxidative stress effects by activating Nrf2 in primary murine macrophages. Primary murine macrophages were treated with ML385 (3 μ M) for 2 h following incubation with cyasterone (100 μ M) for 24 h with or without LPS (100 ng/ml) for 12 h. **A** The expression of Nrf2 was analyzed by fluorescence microscopy. **B–E** Q-PCR and Western blotting were used to detect the mRNA and protein expression levels of NQO-1 and HO-1. **F–G** The ROS content was analyzed by fluorescence microscopy. **H–I** The ROS content was measured by flow cytometry. **J–P** IL-6, IL-1 β , TNF- α , Cox2, NLRP3, pro-caspase-1 and Asc mRNA were determined with Q-PCR. **Q–R** Western blotting was used to detect the protein expression levels of NLRP3 and caspase-1 p10. Data are expressed as mean \pm SD, n = 3, *P < 0.05; **P < 0.01; ***P < 0.001; ****P < 0.0001

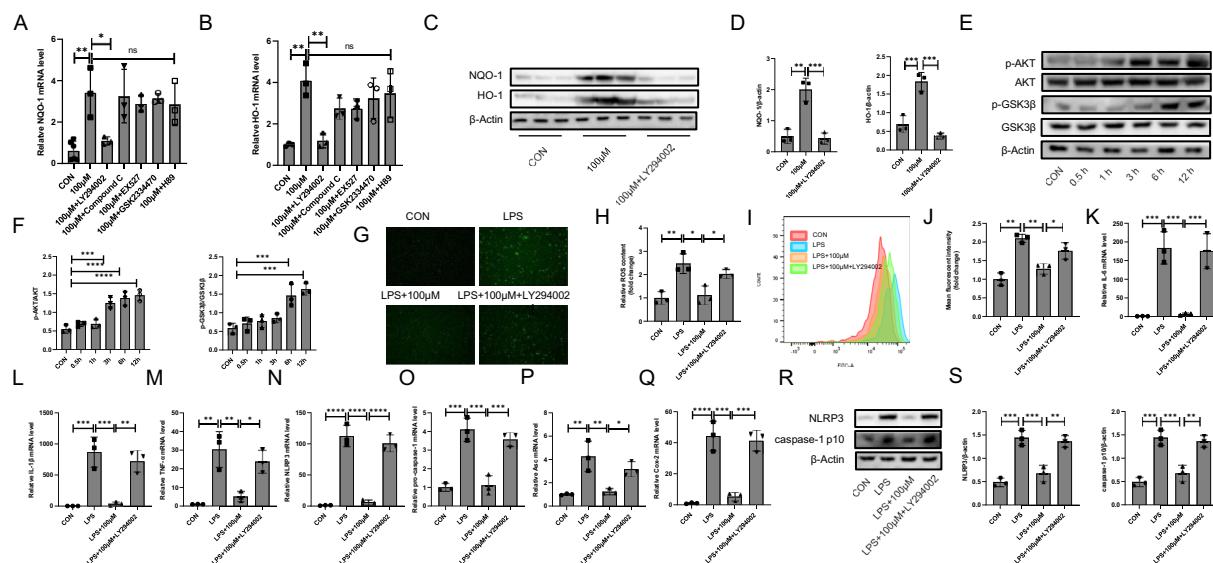


Fig. 5 The AKT (Ser473)/GSK3 β (Ser9) pathway mediates cyasterone induced Nrf2 activation in primary murine macrophages. Primary murine macrophages were treated with LY294002 (10 μ M), Compound C (5 μ M), EX527 (10 μ M), GSK2334470 (1 μ M), H89 (10 μ M), respectively, for 2 h following incubation with cyasterone (100 μ M) for 24 h with or without LPS (100 ng/ml) for 12 h. **A, B** NQO-1 and HO-1 mRNA were determined with Q-PCR. **C, D** Western blotting was used to detect the protein expression levels of NQO-1 and HO-1. **E, F** Primary murine macrophages were treated with cyasterone (100 μ M) for 0, 0.5, 1, 3, 6, 12 h. Western blotting was used to detect the protein expression levels of p-AKT, AKT, GSK3 β and p-GSK3 β . **G, H** The ROS content was analyzed by fluorescence microscopy. **I, J** The ROS content was measured by flow cytometry. **K–Q** IL-6, IL-1 β , TNF- α , Cox2, NLRP3, pro-caspase-1 and Asc mRNA were determined with Q-PCR. **R, S** Western blotting was used to detect the protein expression levels of NLRP3 and caspase-1 p10. Data are expressed as mean \pm SD, n = 3, *P < 0.05; **P < 0.01; ***P < 0.001; ****P < 0.0001

aggregates in response to cyasterone (Fig. 6E–G). Furthermore, cyasterone effectively inhibited LPS-induced cell apoptosis (Fig. 6H, I). These results indicate that cyasterone could against oxidative damage and apoptosis in MLE12 cells.

The AKT (Ser473)/ Nrf2 pathway mediates cyasterone against cell injury in MLE12 cells

To deeper explore whether the inhibition role of cyasterone on oxidative damage in MLE12 cells through the AKT (Ser473)/Nrf2 pathway, we pre-treated MLE12 cells with AKT and Nrf2 inhibitors. The outcomes revealed that LY294002 and ML385 attenuated cyasterone's capacity to alleviate cellular and mitochondrial ROS levels (Fig. 7A–D). Additionally, the JC-1 assay indicated that LY294002 and ML385 hindered the ability of cyasterone in increasing the proportion of JC-1 aggregates (Fig. 7E–G). Furthermore, the impact of cyasterone on inhibiting epithelial cell apoptosis was mitigated by LY294002 and ML385 (Fig. 7H, I).

Cyasterone relieves the CLP-induced ALI via AKT (Ser473)/ GSK3 β (Ser9)/ Nrf2 pathway

To verify whether cyasterone attenuated CLP-induced acute lung injury in mice via the AKT (Ser473)/GSK3 β (Ser9)/Nrf2 pathway, ML385 or LY294002 were injected intraperitoneally 3 h before the injection of cyasterone (Fig. 8A). HE staining results showed that ML385 and LY294002 groups of mice with disorganized lung Histological disorders (Fig. 8B, C). And ML385 and LY294002 reversed the effects of cyasterone in reducing the wet/dry ratio (Fig. 8D). In addition, the effect of cyasterone in decreasing the expression of inflammatory factors (Fig. 8E–H), inhibiting the activation of NLRP3 inflammasome (Fig. 8I–K, N–O), and anti-oxidative stress (Fig. 8L–N, P–T) were reversed by ML385 and LY294002. These results suggest that cyasterone alleviates the CLP-induced ALI via the AKT (Ser473)/ GSK3 β (Ser9)/ Nrf2 pathway (Figs. 8).

Discussion

Our study shows for the first time that cyasterone ameliorates sepsis-related ALI by inhibiting oxidative stress and inflammatory responses. We found that

cyasterone pretreatment attenuated CLP-induced lung histopathological damage and oxidative stress, reduced inflammatory factor secretion, and inhibited NLRP3 inflammasome activation in ALI mice. Meanwhile, cyasterone increased the expression of antioxidant enzymes regulated by AKT(Ser473)/GSK3 β (S9)/Nrf2 activation, decreased ROS content and thus reduced pro-inflammatory cytokine release and NLRP3 inflammasome activation stimulated by LPS in primary mouse peritoneal macrophages (Fig. 9). These results demonstrate that cyasterone may be a potential drug for preventing sepsis-related ALI.

Excessive inflammatory response plays a vital role in the development of ALI. Numerous studies have reported that NLRP3 inflammasomes function critically in ALI [30, 31]. LPS stimulation induces TXNIP binding to NLRP3, leading to NLRP3 inflammasome activation [32]. NLRP3 inflammasomes activation releases large amounts of mature IL-1 β and IL-18, further amplifying the inflammatory response cascade [33]. Our results showed that cyasterone suppressed NLRP3 inflammasomes activation, suggesting that cyasterone protects against sepsis-associated ALI and may be related to inhibiting NLRP3 inflammasomes activation.

Oxidative stress is another essential characteristic of ALI [34]. Our study also showed that cyasterone attenuates oxidative stress in ALI mice and enhances antioxidant mechanisms involving Nrf2 activation. Extensive literature shows that ROS is one of the most vital factors regulating NLRP3 inflammasome activation [8, 9]. Although it was proposed in one study that Nrf2 is required for NLRP3 inflammasomes activation [35], another study showed that Nrf2 limits NLRP3 inflammasomes activation by downregulating ROS content [36]. Our results indicate that cyasterone can promote the expression of Nrf2 downstream antioxidant genes NQO-1 and HO-1 in a concentration-dependent manner, attenuating oxidative stress. Based on these results, we hypothesized that cyasterone could inhibit NLRP3 inflammasome activation by restoring the balance of oxidative and antioxidant mechanisms in ALI.

Normally, Nrf2 exists at low basal levels because the proteasome degrades it soon after synthesis [11]. It has been shown that Nrf2 activation can alleviate ALI in

(See figure on next page.)

Fig. 6 Cyasterone against oxidative damage and apoptosis in MLE12 cells. **A** The effects of the different concentrations of cyasterone (0, 1, 3, 10, 30, 100 and 200 μ M) on cell viability were evaluated. **B–I** MLE12 cells were treated with serial concentrations of cyasterone (10, 30 or 100 μ M) for 24 h with or without LPS (100 ng/ml) for 12 h. **B, C** The ROS content was analyzed by fluorescence microscopy and flow cytometry. **D** MitoSOX (5 μ M) was measured by fluorescence microscopy. **E–G** Mitochondrial membrane potential ($\Delta\Psi$ m, MMP) was measured by flow cytometry and fluorescence microscopy with 5 μ M JC-1. **H, I** The apoptosis of MLE12 cells was detected by flow cytometry. Data are expressed as mean \pm SD, n = 3, *P < 0.05; **P < 0.01; ***P < 0.001; ****P < 0.0001

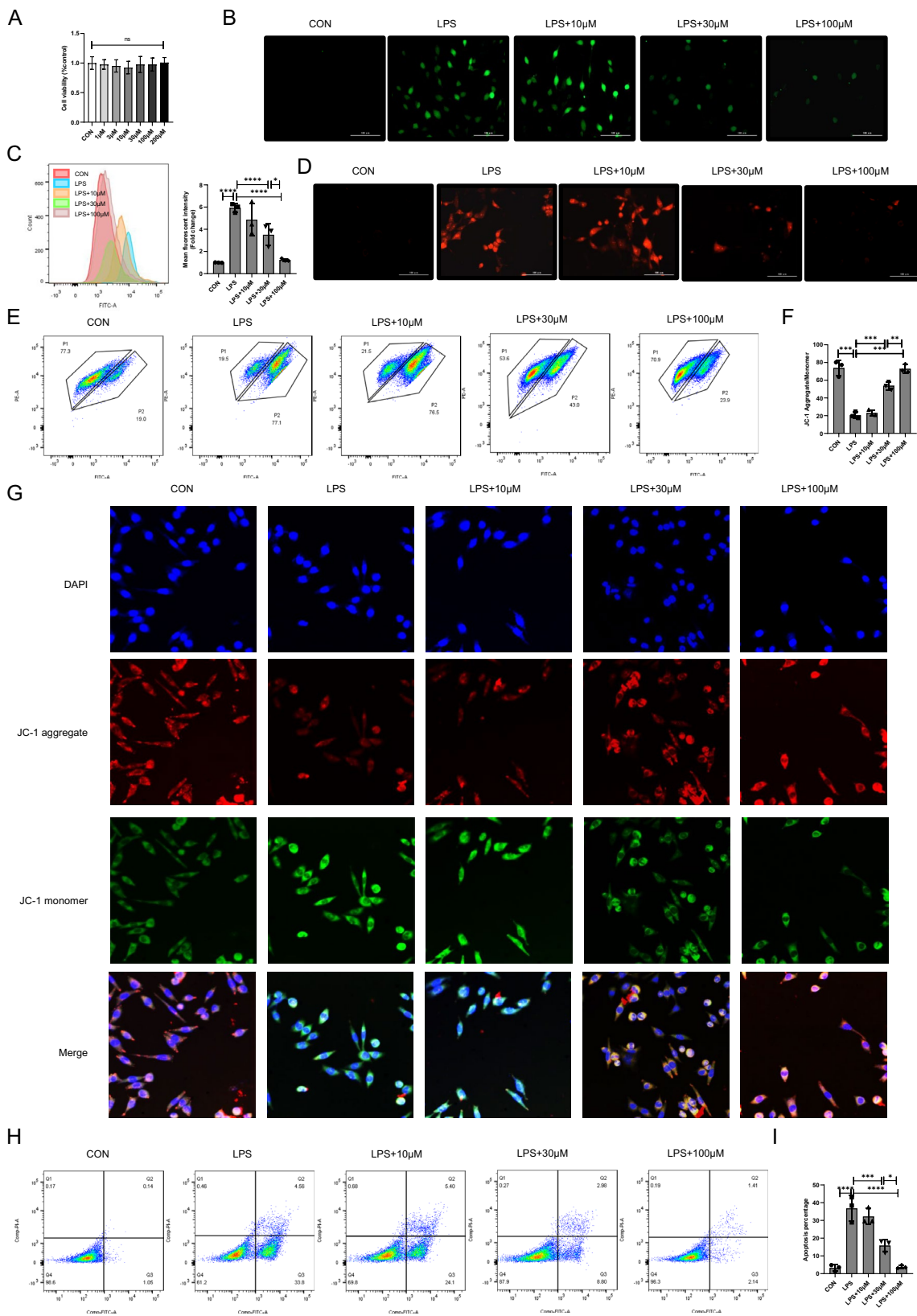


Fig. 6 (See legend on previous page.)

mice [37, 38]. Among them, Keap1, the fundamental mechanism of Nrf2 activation, is the main regulator of Nrf2 activity [39]. Under oxidative stress, the cysteine residues on Keap1 are oxidized, releasing Nrf2 from the Keap1/Nrf2 complex and subsequent translocation to the nucleus [40]. It has also been reported that GSK3 β -mediated regulatory pathways independent of Keap1 have a critical role in ALI induced by severe oxidative stress injury [13]. In addition to the ubiquitinated degradation of Nrf2 protein by phosphorylating specific serine residues of the Nrf2 Neh6 structural domain and forming a degradation domain recognized by the ubiquitin ligase adapter protein β -TrCP [41]. GSK3 β can also export Nrf2 outside the cytoplasm by phosphorylating Fyn [42]. It is reported that sulforaphane can prevent chromium-induced lung injury in rats by activating the AKT/GSK-3 β /Fyn pathway [43]. Another study also showed that melatonin prevented LPS-induced epithelial-mesenchymal transition in human alveolar epithelial cells via the GSK-3 β /Nrf2 pathway [44]. Our results found that cyasterone can upregulate the expression of p-GSK-3 β in a time gradient. Therefore, it is suggested that cyasterone can reduce Nrf2 degradation by inactivating GSK3 β and cyasterone promotes Nrf2 entry into the nucleus, possibly by reducing GSK3 β / β -TrCP-mediated Nrf2 degradation. However, further investigation needs to investigate whether cyasterone can reduce the nuclear export of Nrf2 by inhibiting Fyn kinase.

Multiple upstream signals can activate Nrf2 [27–29], and in this study, we selected inhibitors of SIRT1, AMPK, AKT, PDK and PKA, five important kinases upstream of

Nrf2, and the results showed that inhibition of AKT can suppress the expression of NQO-1 and HO-1. PI3K/AKT is a multifunctional signaling pathway associated with cell proliferation, apoptosis and defense [45]. Mitochondrial quality control has been reported to have a significant role in septic lung oxidative injury through activation of PI3K/AKT pathway [46]. In contrast, LY294002, administered intraperitoneally, exacerbated the sepsis-related ALI [47]. Thus, drugs that enhance AKT activity may be novel agents for preventing sepsis-related lung injury. Our results also indicate that cyasterone can activate AKT time-dependently. Furthermore, the effect of cyasterone in reducing intracellular ROS content and inhibiting NLRP3 inflammasome activation was inhibited after the administration of LY294002.

Cyasterone is an active ingredient extracted from the traditional Chinese medicine *Radix cyathulae* [18]. It was demonstrated that in cancer cells A549 and MGC823, cyasterone blocked EGFR phosphorylation in a concentration-dependent manner, further inhibiting its downstream AKT phosphorylation [48]. However, cyasterone showed relatively high security in three normal human cells (HUVEC, L02, HEK293) [48]. Our results show that cyasterone activates AKT and inactivates GSK3 β to promote its nuclear entry and antioxidant effects in mouse primary peritoneal macrophages.

(See figure on next page.)

Fig. 7 The AKT (Ser473)/Nrf2 pathway mediates cyasterone against cell injury in MLE12 cells. **A–I** MLE12 cells were treated with ML385 (3 μ M) or LY294002 (10 μ M) for 2 h following incubation with cyasterone (100 μ M) for 24 h with or without LPS (100 ng/ml) for 12 h. **A–C** The ROS content was analyzed by fluorescence microscopy and flow cytometry. **D** MitoSOX (5 μ M) was measured by fluorescence microscopy. **E–G** Mitochondrial membrane potential ($\Delta\Psi_m$, MMP) was measured by flow cytometry and fluorescence microscopy with 5 μ M JC-1. **H, I** The apoptosis of MLE12 cells was detected by flow cytometry. Data are expressed as mean \pm SD, n = 3, *P < 0.05; **P < 0.01; ***P < 0.001; ****P < 0.0001

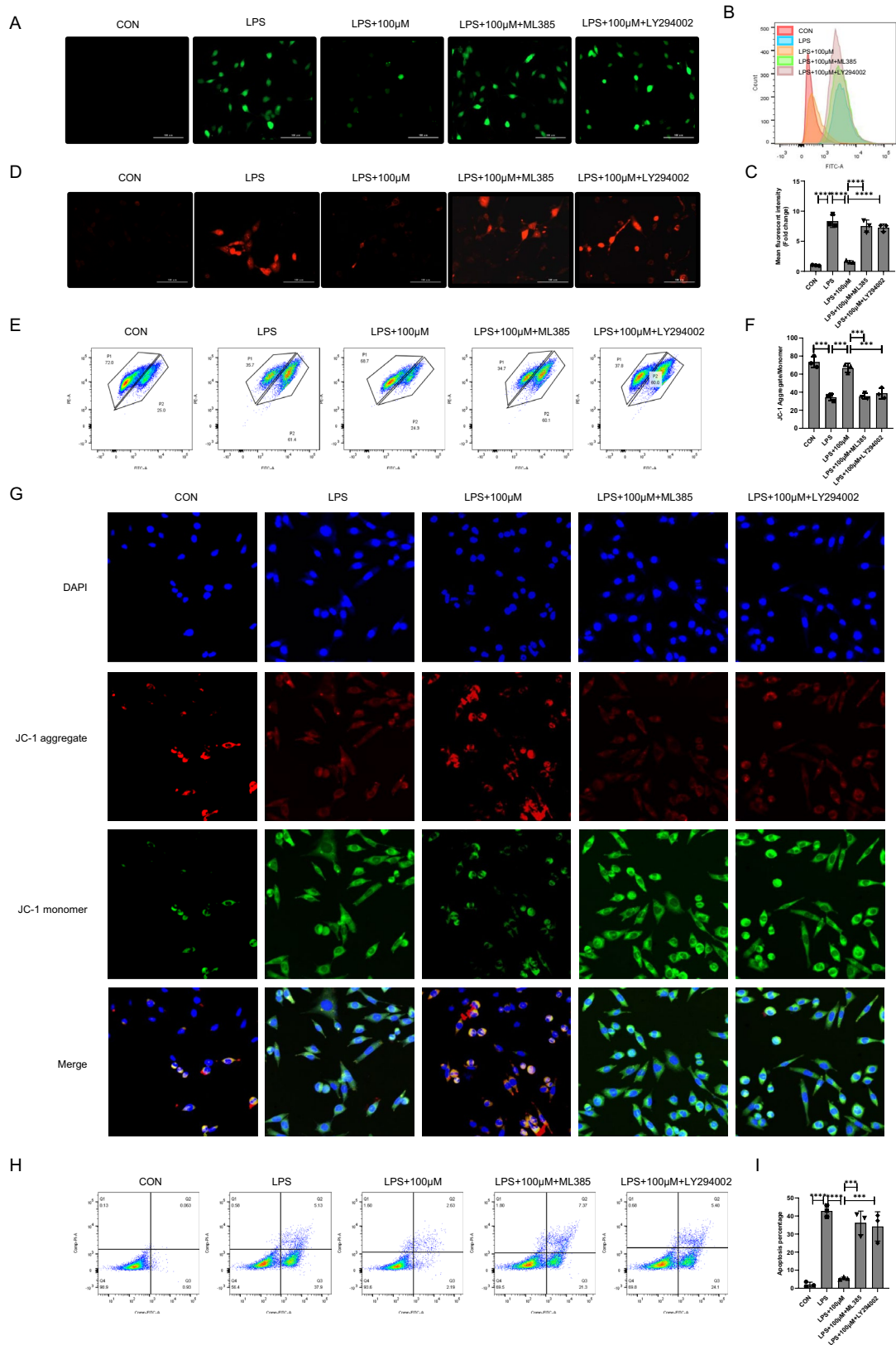


Fig. 7 (See legend on previous page.)

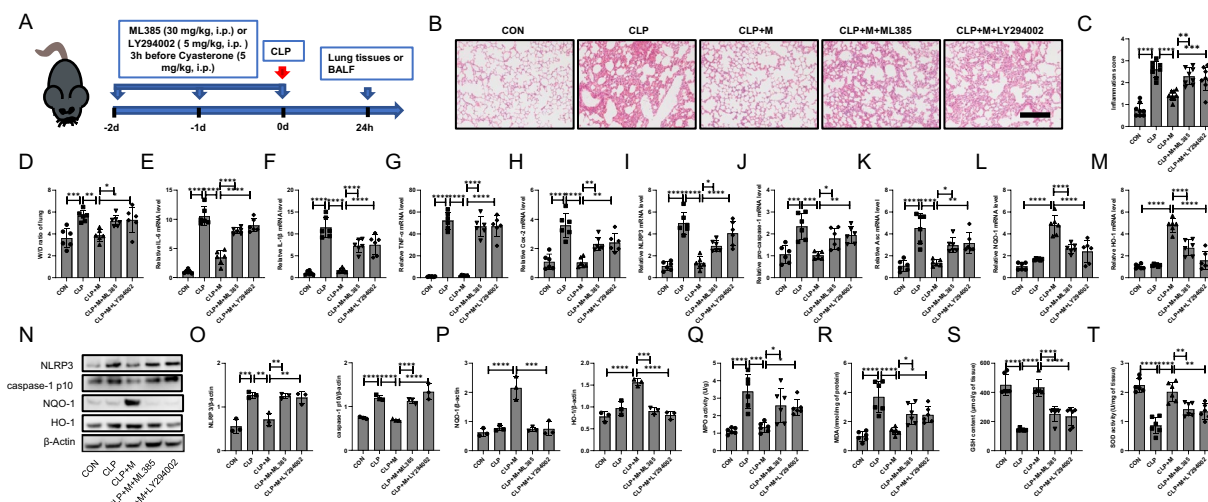


Fig. 8 Cyasterone relieves the CLP-induced ALI by AKT (Ser473)/GSK3β (Ser9)/Nrf2 pathway. **A** ML385 (30 mg/kg) or LY294002 (5 mg/kg) were injected intraperitoneally 3 h before the injection of cyasterone (5 mg/kg). **B, C** HE staining and lung inflammation score were used to detect the lung histopathological changes. Bars represent 100 μm. **D** Lung W/D ratio was measured to determine lung permeability. **E–M** IL-6, IL-1β, TNF-α, Cox2, NLRP3, pro-caspase-1, Asc, NQO-1 and HO-1 mRNA in the lungs were determined with Q-PCR. **N–P** Western blotting was used to detect the protein expression levels of NLRP3, caspase-1 p10, NQO-1 and HO-1. **Q–T** MPO activity, MDA content, GSH content and SOD activity in lung tissue were determined. Data are expressed as mean ± SD, n=6–8, *P < 0.05; **P < 0.01; ***P < 0.001; ****P < 0.0001

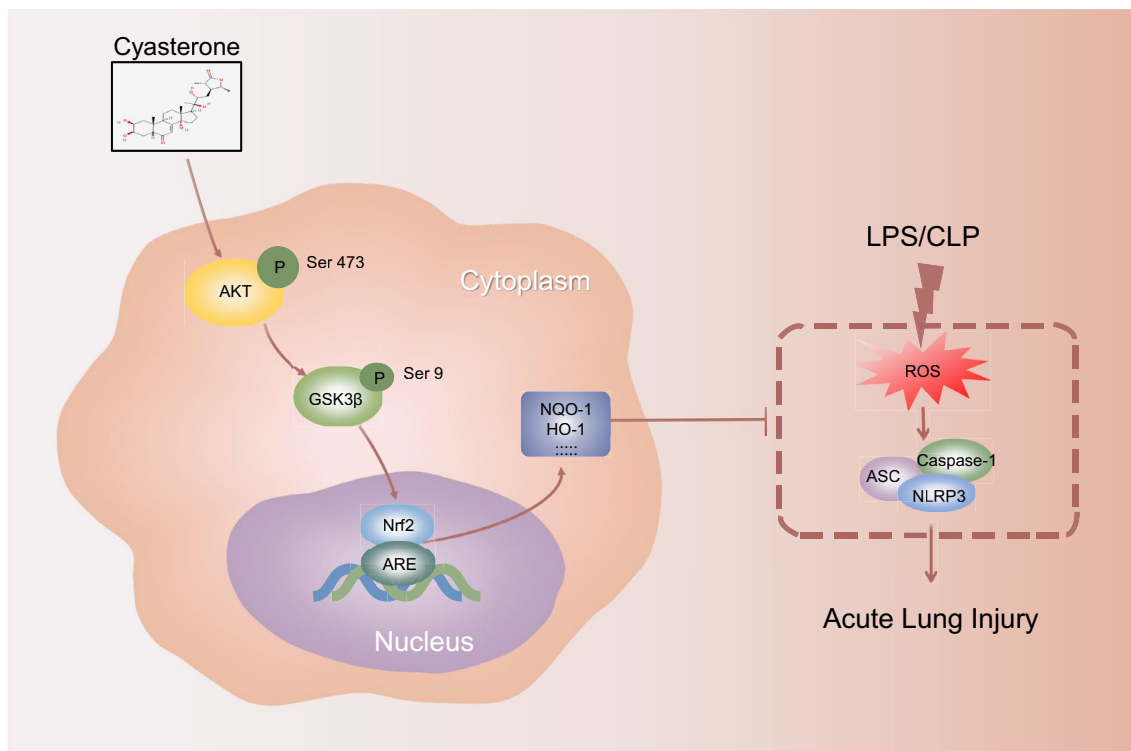


Fig. 9 Schematic representation of the protective effect of cyasterone on CLP-induced ALI via AKT (Ser473)/GSK3β (Ser9)/Nrf2 axis. Cyasterone pretreatment activates AKT and GSK3β, promotes Nrf2 nuclear translocation, increases the expression of antioxidant enzymes such as NQO-1 and HO-1, thereby reducing ROS content, inhibiting NLRP3 inflammasome activation in macrophages, and exerts a mitigating effect on CLP-induced ALI

Conclusions

Our data reveal for the first time that cyasterone protects against CLP-induced ALI in mice. Cyasterone attenuates inflammation and oxidative stress in ALI mice, mainly attributed to the anti-inflammatory and antioxidant properties of cyasterone via AKT (Ser473)/GSK3 β (Ser9)-mediated Nrf2 activation in macrophages and alveolar epithelial cell. These results suggest that cyasterone may be a potential drug candidate for preventing sepsis-induced ALI.

Abbreviations

ALI	Acute lung injury
ARDS	Acute respiratory distress syndrome
CLP	Cecal ligation perforation
LPS	Lipopolysaccharide
Nrf2	Nuclear factor erythroid2-related factor 2
AKT	Protein kinase A
GSK3 β	Glycogen synthase kinase-3 β
NLRP3	NOD-like receptor thermal protein domain associated protein 3
ROS	Reactive oxygen species
TXNIP	Thioredoxin-interacting protein
Trx	Thioredoxin
IL	Interleukin
TNF- α	Tumor necrosis factor- α
Cox-2	Cyclooxygenase-2
ARE	Antioxidant response element
BALF	Bronchoalveolar lavage fluid

Supplementary Information

The online version contains supplementary material available at <https://doi.org/10.1186/s13020-023-00837-2>.

Additional file 1: Figure S1. The effects of cyasterone and dexamethasone on alleviating CLP-induced ALI in mice showed no significant difference. **A** Cyasterone (5 mg/kg) or dexamethasone (5 mg/kg) was administered intraperitoneally to compare their effects on CLP-induced ALI. **B, C** HE staining and lung inflammation score were used to detect the lung histopathological changes. Bars represent 100 μ m. **D** Lung W/D ratio was measured to determine lung permeability. **E** The number of macrophages in BALF was measured. **F** MPO activity in lung tissue were determined. **G, H** IL-1 β , TNF- α in BALF were determined with ELISA. **I-N** IL-6, IL-1 β , TNF- α , NLRP3, pro-caspase-1 and Asc mRNA in the lungs were determined with Q-PCR. **O, P** Western blotting was used to detect the protein expression levels of NLRP3 and caspase-1 p10. Data are expressed as mean \pm SD, n = 6–8, *P<0.05; **P<0.01; ***P<0.001; ****P<0.0001.

Acknowledgements

Thanks to all the teachers and students in the lab for their contributions to this study.

Author contributions

ML and DX design of the work; ST, WX, LD, XH, LH and XZ the acquisition, analysis; QH, RQ and TZ interpretation of data; QZ, XS and YL the creation of new software used in the work; ML, DX, WL and LR have drafted the work or substantively revised it; WX revision of this paper. All authors read and approved the final manuscript.

Funding

This work was supported by the Fundamental Research Funds for the Central Universities of Central South University [Grant Number: CX20210344, 2023ZZTS0862, CX20230307]; Natural Science Foundation of Hunan Province, China [Grant Numbers: 2020JJ5828, 2020JJ4773, 2021JJ30899, 2022JJ40293]; The Open-End Fund for the Valuable and Precision

Instruments of Central South University [Grant Number: CSUZC202251]; The Fund for the State Key Laboratory of Hunan Province, China [Grant Number: 2017TP1004]; This work was supported by the National Natural Science Foundation of China (Grant Numbers:82100084, 81500056 and 82170853).

Availability of data and materials

All data generated or analyzed during this study are included in this published article.

Declarations

Ethics approval and consent to participate

The animal study protocol was approved by the Laboratory Animal Welfare and Ethical Committee of Central South University (Approval No. CSU-2022-0095).

Consent for publication

Not applicable.

Competing interests

The authors declare that they have no competing interests.

Author details

¹Department of Community Nursing, Xiangya Nursing School, Central South University, Changsha 410013, China. ²Occupational Disease Department, Hunan Prevention and Treatment Institute for Occupational Diseases, Changsha 410013, China. ³Clinical Nursing Teaching and Research Section, The Second Xiangya Hospital, Central South University, Changsha 410013, China.

Received: 13 June 2023 Accepted: 15 September 2023

Published online: 19 October 2023

References

- Fleischmann C, et al. Assessment of global incidence and mortality of hospital-treated sepsis current estimates and limitations. *Am J Respir Crit Care Med*. 2016;193(3):259–72.
- Truwit JD, et al. Effect of vitamin C infusion on organ failure and biomarkers of inflammation and vascular injury in patients with sepsis and severe acute respiratory failure: the CITRIS-ALI randomized clinical trial. *JAMA*. 2019;322(13):1261–70.
- Mokra D. Acute lung injury—from pathophysiology to treatment. *Physiol Res*. 2020;69(Suppl 3):S353.
- Gattinoni L, et al. The future of mechanical ventilation: lessons from the present and the past. *Crit Care*. 2017;21:1–11.
- Network ARDS. Ventilation with lower tidal volumes as compared with traditional tidal volumes for acute lung injury and the acute respiratory distress syndrome. *N Engl J Med*. 2000;342(18):1301–8.
- Areschoug T, Gordon S. Pattern recognition receptors and their role in innate immunity: focus on microbial protein ligands. *Trends Innate Immun*. 2008;15:45–60.
- Kim SY, et al. Pro-inflammatory hepatic macrophages generate ROS through NADPH oxidase 2 via endocytosis of monomeric TLR4–MD2 complex. *Nat Commun*. 2017;8(1):2247.
- Luo T, et al. Corilagin restrains NLRP3 inflammasome activation and pyroptosis through the ROS/TXNIP/NLRP3 pathway to prevent inflammation. *Oxid Med Cell Longev*. 2022;2022(1):1652244.
- Minutoli L, et al. ROS-mediated NLRP3 inflammasome activation in brain, heart, kidney, and testis ischemia/reperfusion injury. *Oxid Med Cell Longev*. 2016;2016(1):2183026.
- Ma Q. Role of nrf2 in oxidative stress and toxicity. *Annu Rev Pharmacol Toxicol*. 2013;53:401–26.
- Tonelli C, Chio IIC, Tuveson DA. Transcriptional regulation by Nrf2. *Antioxid Redox Signal*. 2018;29(17):1727–45.
- Bellezza I, et al. Nrf2-Keap1 signaling in oxidative and reductive stress. *Biochim Biophys Acta (BBA)-Mol Cell Res*. 2018;1865(5):721–33.
- Liao S, et al. A novel compound DBZ ameliorates neuroinflammation in LPS-stimulated microglia and ischemic stroke rats: Role of Akt (Ser473)/GSK3 β (Ser9)-mediated Nrf2 activation. *Redox Biol*. 2020;36:101644.

14. Huang Y, et al. Review of traditional uses, botany, chemistry, pharmacology, pharmacokinetics, and toxicology of radix cyathulae. *Chin Med.* 2019;14:1–16.
15. Li L, et al. BaZiBuShen alleviates altered testicular morphology and spermatogenesis and modulates Sirt6/P53 and Sirt6/NF- κ B pathways in aging mice induced by D-galactose and NaNO₂. *J Ethnopharmacol.* 2021;271:113810.
16. Liu S-J, et al. Mechanism of Cyathulae Radix in treatment of knee osteoarthritis based on metabolomics. *Zhongguo Zhong yao za zhi= Zhongguo Zhongyao Zazhi China J Chin Mater Med.* 2022;47(22):6199–206.
17. Kayani WK, et al. Evaluation of ajuga bracteosa for antioxidant, anti-inflammatory, analgesic, antidepressant and anticoagulant activities. *BMC Complement Altern Med.* 2016;16(1):375.
18. Okuzumi K, et al. Structure elucidation of cyasterone stereoisomers isolated from cyathula officinalis. *Org Biomol Chem.* 2005;3(7):1227–32.
19. Teng L, et al. Cyasterone inhibits IL-1 β -mediated apoptosis and inflammation via the NF- κ B and MAPK signaling pathways in rat chondrocytes and ameliorates osteoarthritis in vivo. *Chin J Nat Med.* 2023;21(2):99–112. [https://doi.org/10.1016/S1875-5364\(23\)60388-7](https://doi.org/10.1016/S1875-5364(23)60388-7).
20. Zhu J, et al. Cyasterone accelerates fracture healing by promoting MSCs migration and osteogenesis. *J Orthop Transl.* 2021;28:28–38. <https://doi.org/10.1016/j.jot.2020.11.004>.
21. Wu XL, et al. The protective effects of the supercritical-carbon dioxide fluid extract of chrysanthemum indicum against lipopolysaccharide-induced acute lung injury in mice via modulating Toll-like receptor 4 signaling pathway. *Med Inflamm.* 2014;2014:246407. <https://doi.org/10.1155/2014/246407>.
22. Al-Harbi NO, et al. Dexamethasone attenuates Lps-induced acute lung injury through inhibition of NF- κ B, COX-2, and pro-inflammatory mediators. *Immunol Investig.* 2016;45(4):349–69. <https://doi.org/10.3109/08820139.2016.1157814>.
23. Rittirsch D, et al. Immunodissection of experimental sepsis by cecal ligation and puncture. *Nat Protoc.* 2009;4(1):31–6. <https://doi.org/10.1038/nprot.2008.214>.
24. Jones KD, Urisman A. Histopathologic approach to the surgical lung biopsy in interstitial lung disease. *Clin Chest Med.* 2012;33(1):27–40.
25. Tabatabaei MS, Ahmed M. Enzyme-linked immunosorbent assay (ELISA). In: *Cancer cell biology: methods and protocols.* Springer; 2022. p. 115–34.
26. Ward PA. Oxidative stress: acute and progressive lung injury. *Ann N Y Acad Sci.* 2010;1203(1):53–9.
27. Dang R, et al. Edaravone ameliorates depressive and anxiety-like behaviors via Sirt1/Nrf2/HO-1/Gpx4 pathway. *J Neuroinflammation.* 2022;19(1):1–29.
28. Park SY, et al. Schizandrin C exerts anti-neuroinflammatory effects by upregulating phase II detoxifying/antioxidant enzymes in microglia. *Int Immunopharmacol.* 2013;17(2):415–26.
29. Duan J, et al. Protective effect of butin against ischemia/reperfusion-induced myocardial injury in diabetic mice: involvement of the AMPK/GSK-3 β /Nrf2 signaling pathway. *Sci Rep.* 2017;7(1):41491.
30. Yang H, et al. Oridonin protects LPS-induced acute lung injury by modulating Nrf2-mediated oxidative stress and Nrf2-independent NLRP3 and NF- κ B pathways. *Cell Commun Signal.* 2019;17(1):62.
31. Zhang J, et al. Loganin alleviates sepsis-induced acute lung injury by regulating macrophage polarization and inhibiting NLRP3 inflammasome activation. *Int Immunopharmacol.* 2021;95:107529.
32. Li N, et al. STING-IRF3 contributes to lipopolysaccharide-induced cardiac dysfunction, inflammation, apoptosis and pyroptosis by activating NLRP3. *Redox Biol.* 2019;24:101215.
33. Paget C, et al. Specific NLRP3 inflammasome assembling and regulation in neutrophils: relevance in inflammatory and infectious diseases. *Cells.* 2022;11(7):1188.
34. Esmaili Y, et al. Targeting autophagy, oxidative stress, and ER stress for neurodegenerative diseases treatment. *J Controll Release.* 2022;345:147.
35. Sogawa Y, et al. Infiltration of M1, but not M2, macrophages is impaired after unilateral ureter obstruction in Nrf2-deficient mice. *Sci Rep.* 2017;7(1):1–11.
36. Liu X, et al. Nuclear factor E2-related factor-2 negatively regulates NLRP3 inflammasome activity by inhibiting reactive oxygen species-induced NLRP3 priming. *Antioxid Redox Signal.* 2017;26(1):28–43.
37. Kong L, et al. Sitagliptin activates the p62-Keap1-Nrf2 signalling pathway to alleviate oxidative stress and excessive autophagy in severe acute pancreatitis-related acute lung injury. *Cell Death Dis.* 2021;12(10):928.
38. Yang W, et al. Maresin1 protect against ferroptosis-induced liver injury through ROS inhibition and Nrf2/HO-1/GPX4 activation. *Front Pharmacol.* 2022;13:1098.
39. Lu MC, et al. The Keap1-Nrf2-ARE pathway as a potential preventive and therapeutic target: an update. *Med Res Rev.* 2016;36(5):924–63.
40. Baird L, Yamamoto M. The molecular mechanisms regulating the KEAP1-NRF2 pathway. *Mol Cell Biol.* 2020;40(13):e00099-e120.
41. Hsieh C-H, et al. An innovative NRF2 nano-modulator induces lung cancer ferroptosis and elicits an immunostimulatory tumor microenvironment. *Theranostics.* 2021;11(14):7072.
42. Li T, et al. BP5 alleviates endotoxemia-induced acute lung injury by activating Nrf2 via dual regulation of the Keap1-Nrf2 interaction and the Akt (Ser473)/GSK3 β (Ser9)/Fyn pathway. *Free Radical Biol Med.* 2022;193:304–18.
43. Lv Y, et al. Sulforaphane prevents chromium-induced lung injury in rats via activation of the Akt/GSK-3 β /Fyn pathway. *Environ Pollut.* 2020;259:113812.
44. Ding Z, et al. Melatonin prevents LPS-induced epithelial-mesenchymal transition in human alveolar epithelial cells via the GSK-3 β /Nrf2 pathway. *Biomed Pharmacother.* 2020;132:110827.
45. Ediriweera MK, Tennekoon KH, Samarakoon SR. Role of the PI3K/AKT/mTOR signaling pathway in ovarian cancer: biological and therapeutic significance. *Semin Cancer Biol.* 2019;59:147.
46. Shi J, et al. PI3K/Akt pathway-mediated HO-1 induction regulates mitochondrial quality control and attenuates endotoxin-induced acute lung injury. *Lab Invest.* 2019;99(12):1795–809.
47. Li R, Ren T, Zeng J. Mitochondrial coenzyme Q protects sepsis-induced acute lung injury by activating PI3K/Akt/GSK-3 β /mTOR pathway in rats. *BioMed Res Int.* 2019;2019(1):5240898.
48. Lu X, et al. Anti-proliferation effects, efficacy of cyasterone in vitro and in vivo and its mechanism. *Biomed Pharmacother.* 2016;84:330–9.

Publisher's Note

Springer Nature remains neutral with regard to jurisdictional claims in published maps and institutional affiliations.

Ready to submit your research? Choose BMC and benefit from:

- fast, convenient online submission
- thorough peer review by experienced researchers in your field
- rapid publication on acceptance
- support for research data, including large and complex data types
- gold Open Access which fosters wider collaboration and increased citations
- maximum visibility for your research: over 100M website views per year

At BMC, research is always in progress.

Learn more biomedcentral.com/submissions

